ORIGINAL PAPER

A quartz crystal microbalance study of the kinetics of interaction of benzotriazole with copper

F. M. Al Kharafi · A. M. Abdullah ·
B. G. Ateya

Abstract The kinetics of interaction of benzotriazole ($C_6H_5N_3$, BTAH) with the surface of copper in salt water were studied using an electrochemical quartz crystal microbalance and X-ray photoelectron spectroscopy (XPS). Upon injecting BTAH into the electrolyte, three regions appear in the time response of the microbalance. Region I (at short time of few minutes), exhibits rapid linear growth of mass with time, which is attributed to the formation of a protective Cu(I)BTA complex. Region II reveals attachment of BTAH at a slower rate onto the inner Cu(I)BTA complex. Region III is a plateau indicating that the BTAH film attains an equilibrium mass and thickness, which increase with the concentration of BTAH. The intensity of the N1s peak in the XPS spectra increases with the time of immersion, indicating more BTAH on the surface. The results suggest a duplex inhibitor film composed of an inner thin layer of Cu(I)BTA and an outer layer of physically adsorbed BTAH which increases in thickness with time and BTAH concentration. They also offer an explanation for the much documented findings of simultaneous increase of the polarization resistance and decrease of double layer capacity with inhibitor concentration and time of immersion.

Keywords Benzotriazole · Copper · Corrosion inhibitor · Duplex film · Quartz crystal microbalance

F. M. Al Kharafi (✉) · A. M. Abdullah · B. G. Ateya
Chemistry Department, Faculty of Science, University
of Kuwait, P.O. Box 5969, Safat 13060, Kuwait
e-mail: fayzah@aas.com.kw

B. G. Ateya
e-mail: bgateya@yahoo.com

1 Introduction

Benzotriazole ($C_6H_5N_3$, BTAH) has been extensively studied as an inhibitor for the corrosion of copper and many of its alloys [1–16], for dezincification of brass [17, 18] and as additive in the etching [19], electrodeposition [20–22] and in the chemical mechanical polishing of copper [23–25]. It has also been reported to inhibit the corrosion of iron [26–28], cobalt [29], zinc [30], and nickel [28] and to enhance the resistance of tin bronze to oxidation in air [31]. The remarkable inhibiting efficiency of BTAH is attributed to adsorption [32–34] and complex formation [34–38], i.e.,

$$BTAH + Cu = BTAH{:}Cu \qquad (1)$$

$$BTAH + Cu^+ = Cu(I)BTA + H^+, \qquad (2)$$

where BTAH : Cu refers to adsorbed BTAH and Cu(I)BTA is a protective complex.

Most previous studies were concerned with the inhibiting efficiency and characterization of the films grown on the metallic surface after sufficiently long times [4, 13]. The kinetics of interaction of BTAH with the surface of copper have not attracted much attention. This is believed to be due to the complexity of the kinetic behavior and also the difficulty of performing such measurements.

It is now possible to follow such behavior in situ and in real time using an electrochemical quartz crystal microbalance (EQMB). This balance utilizes the piezoelectric properties of quartz crystals [39]. Crystals which acquire a charge when compressed, twisted or distorted are said to be piezoelectric. A quartz crystal has a well-defined natural frequency, f (defined by its shape and size) at which it prefers to oscillate. Loss or gain of mass from the surface of the crystal changes the frequency f. The change in mass

(Δm) and in the oscillation frequency (Δf) are related by the following equation [39, 40]:

$$\Delta f = -2\Delta m f^2/A(\mu\rho_q)^{1/2} = -C_f\Delta m, \qquad (3)$$

where f is the oscillation frequency of the quartz crystal (9 MHz), Δm is the elastic mass change (g), A is the electrode area (0.196 cm^2), ρ_q is the density of quartz (2.648 g cm^{-3}), and μ is the shear modulus of the crystal (2.947×10^{11} g cm^{-1} s^{-2}). The constant C_f is the integrated EQMB sensitivity, which has a value of 0.9363 Hz ng^{-1}. This equation can then be simplified to

$$\Delta m = -1.068\ \Delta f, \qquad (4)$$

where Δm is in nano grams and f is in Hz. Equation 4 is valid for small evenly distributed elastic masses added to or taken from the crystal surface and when the mass change is within 2% of the mass of the quartz crystal [39, 40]. Many factors affect the accuracy of measurements of the EQMB such as surface roughness, density and viscosity of the liquid in contact with the crystal [40]. The EQMB has been used in studies of corrosion and protection of metals [13–15, 41–47].

The objective of this paper is to analyze the kinetics of interaction of BTAH with the surface of copper in salt water. This is pursued using an electrochemical quartz microbalance (EQMB). This approach enables one to follow the kinetics of the process in situ and in real time.

2 Experimental details

The quartz crystal used in these experiments was an AT-cut disk of area 0.196 cm^2 (diameter 2.5 mm) and its nominal resonant frequency was 9 MHz. On both sides, a 3,000 Å thick layer of Au was sputtered on a 100 Å Ti layer. The crystal holder is a well-type shaped holder (QA-CL4) which was obtained from Seiko EG&G Co. Ltd. The EQMB (QCM922 from Seiko EG&G Co. Ltd) was coupled with a Gamry PCI4 Potentiostat. All measurements were performed in 3.5% NaCl under free corrosion conditions in a conventional three-electrode cell. Copper was electroplated from an acid sulfate bath and inspected microscopically to ensure a uniform layer. The copper coated quartz crystal was immersed in the electrolyte for 1 h before the injection of BTAH. To achieve a certain concentration of BTAH, a small volume of a concentrated solution of BTAH in 3.5% NaCl was injected into the electrolyte and stirred rapidly. The surfaces of the electrodes were examined using XPS, VG SCIENTIFIC 200 Spectrometer (UK).

3 Results and discussion

Figure 1 is an illustrative example of the time variation of the changes in frequency (Δf) and mass (Δm in µg) of the

quartz crystal. The initial decrease in mass and increase in frequency refer to the corrosion of copper (before injection of BTAH). The corrosion of copper in this medium is a complex process that leads to the formation of soluble and insoluble corrosion products such as $CuCl_2^-$, $CuCl_2$, $CuCl$, Cu_2O, $Cu_2(OH)_3Cl$,...etc. [48, 49]. While the solid corrosion products remain on the surface, the soluble products pass into the electrolyte leading to a decrease in the mass of the metal. The overall rate of this process can be determined from the slope of the linear part of the mass change, i.e.,

$$\text{corrosion rate} = -\frac{\partial \Delta m}{\partial t}. \qquad (5)$$

The results in Fig. 1 yield a corrosion rate of about 0.008 µg s^{-1} which amounts to 1.26×10^{-10} mole s^{-1} (assuming the product is Cu$^+$). The amount of copper ions that passed into the corrosive medium as a result of the corrosion reaction before injecting BTAH (27.4 µg) amounts to about 4.25×10^{-7} mole of Cu$^+$.

3.1 Injection of BTAH

Upon injection of BTAH into the electrolyte, the trends of Δf and Δm are reversed quite rapidly, indicating an increase in the mass of the copper layer on the quartz crystal. This is attributed to the attachment of BTAH onto the copper surface and the formation of the protective Cu(I)BTAH complex (see Eqs. 1, 2). There is strong evidence that the corrosion rate of copper in the presence of BTAH is negligibly small compared to that in its absence [1–16]. Had BTAH merely stopped the corrosion reaction, one would have observed a constant mass and constant frequency after addition of BTAH. Such a behavior has been recently reported for copper in sulfuric acid upon injection of 5-mercapto-1-phenyl tetrazole (5MPhTT), where the mass of copper remained constant for about 10,000 s [47]. The fact that Δm in the present work increased rapidly with time indicates that BTAH was attached to the copper surface at a high rate. Three regions can be identified in the course of time variation of Δm and Δf, see Fig. 1.

3.1.1 Region I

Immediately following the addition of BTAH (to establish a concentration of 5×10^{-4} M), there is a rapid linear increase of mass with time. This is defined as Region I. This region lasts for about 130 s in Fig. 1 and is associated with a mass gain of about 6 µg which corresponds to

Fig. 1 Changes of resonant frequency (**a**) and mass of copper (**b**) in 3.5% NaCl before and after injection of BTAH into the electrolyte to establish a concentration of 5×10^{-4} M BTAH. The *vertical dashed line* marks the time of injection of BTAH
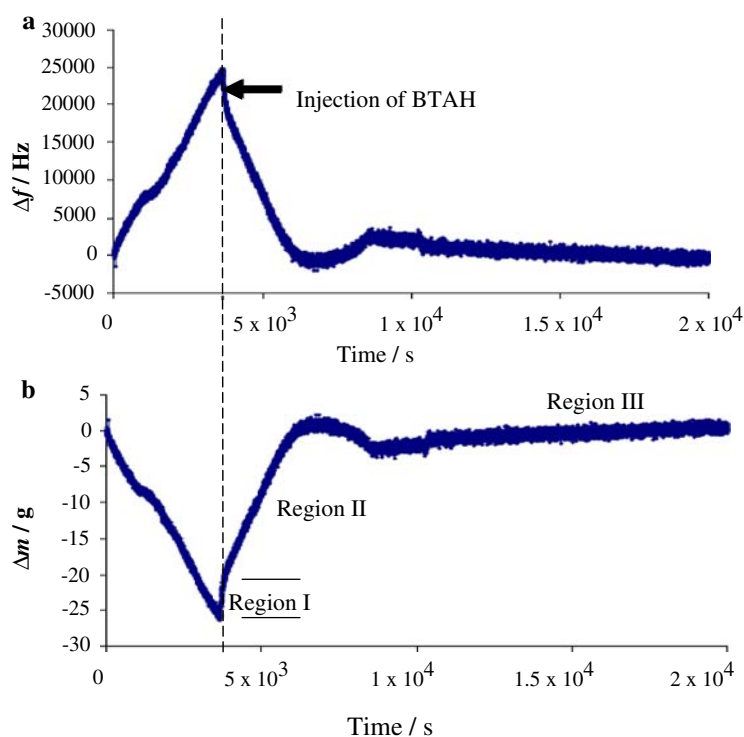
5×10^{-8} mole of BTAH. The protective complex Cu(I)BTA forms readily in view of the presence of Cu$^+$ ions on the surface (e.g., Cu$_2$O). These Cu$^+$ ions remain on the metal surface, before and after their reaction with BTAH and do not cause mass change. Hence, the increase in mass is solely attributed to attachment of BTAH molecules onto the surface. The fact that Region I is linear indicates that the rapid attachment of BTAH onto the surface and the formation of the Cu(I)BTA complex readily occur on empty sites on the copper surface.

The area of a flatly oriented BTAH molecule is estimated at 38.2 Å^2 [13]. Assuming BTAH accumulates uniformly on the copper surface in a flat orientation, at the end of Region I the protective film of BTAH is about 590 layers thick. Taking the thickness of a BTAH molecule to be about 0.92 Å [13] the protective film is estimated to be about 540 Å at the end of Region 1.

The rate of accumulation of BTAH onto the surface can be obtained from the slope of the line in Region I. The value of this slope is 4.61×10^{-2} μg s^{-1} in Fig. 1, which is equivalent to 3.87×10^{-10} mole of BTAH adsorbed on the copper surface per second.

3.1.2 Regions II and III

Region II also shows linear increase of mass with time, at a much lower rate, under the conditions of Fig. 1. The rate of accumulation of BTAH on the surface in Region II

amounts to 9.2×10^{-3} μg s^{-1}, which is about fivefold slower than in Region I (4.61×10^{-2} μg s^{-1}). Region II extends for about 40 min which is much longer than Region I. The mass gain during Region II is about 20 μg which corresponds to about 1.68×10^{-7} moles of BTAH. This is about threefold greater than the mass gain in Region I. Region II is attributed to further attachment of BTAH onto the surface, albeit at a slower rate. By the end of Region II in Fig. 1, the mass of BTAH attached to the copper surface is 27.4 μg, which amounts to 0.23 μmol of BTAH. This is only a small fraction (about 0.5%) of the BTAH that was injected in the electrolyte.

The BTAH that is attached onto the surface in Region II is involved in one or both of the following processes:

1. Formation of more of the protective complex Cu(I)BTA. This process requires diffusion of Cu$^+$ or BTAH through the Cu(I)BTA film that formed in Region I.

2. Attachment of BTAH onto the Cu(I)BTA film, via physical adsorption, without forming Cu(I)BTAH. This might be due van der Waal forces or pi stacking caused by the many pi electron pairs in the BTAH molecule, which is common in similarly conjugated systems [50, 51].

The increase in mass in Region II cannot be readily attributed to the formation of more of the protective Cu(I)BTA complex on the surface. Further growth of t1he Cu(I)BTA film requires outward diffusion of copper ions

through the Cu(I)BTA film (which formed during Region I) to react with BTAH on the surface. In this case, diffusion through the film would be the slow step which requires dependence of mass on the square root of time, i.e., a parabolic rate law. As the film grows linearly with time in Region II, this possibility is excluded. Consequently, Region II is attributed to attachment of more BTAH onto the Cu(I)BTA film formed during Region I, rather than to the formation of more of the complex Cu(I)BTA.

Beyond Region II, the mass remains essentially constant independent of time, Region III. This indicates that the film has attained an equilibrium thickness under this set of conditions. The film has a limiting mass of 27.4 μg under the conditions of Fig. 1, which corresponds to a thickness of about 0.250 μm.

3.1.3 Effects of BTAH concentration

The corresponding results in the presence of higher concentrations of BTAH are shown in Figs. 2 and 3 for 5 and 10 mM BTAH, respectively. The three regions are seen in all the figures. The mass of BTAH attached to the copper surface during Region I amounts to 6 μg (in Figs. 1, 2, 3) which is independent of the concentration of BTAH in the

electrolyte. It is shown above that this mass is sufficient to form a film of the complex Cu(I)BTA with a thickness of about 540 Å.

As the concentration of BTAH in the electrolyte increases, Region II acquires a sigmoidal shape while the plateau of Region III increases. The complex behavior shown in Region II does not follow the parabolic rate law under any concentration, and hence is not attributed to a diffusional process. The limiting values of Δm at the plateau of Region III are 27.4, 63.4, and 136.3 μg, for 5×10^{-4}, 5×10^{-3}, and 1×10^{-2} M BTAH, respectively. The mass gain of 63.4 μg (plateau in Fig. 2) corresponds to about 5.3×10^{-7} mole of BTAH which is more than all the Cu$^+$ ions that resulted from the corrosion reaction before injecting BTAH(4.25×10^{-7} mole). Since only a fraction of these Cu$^+$ ions remains on the copper surface during free corrosion, it follows that the amount of BTAH attached to the surface in Region II is much more than needed to form the complex Cu(I)BTAH. Coupled with the linear increase of mass with time, this suggests that BTAH adsorbs onto the Cu(I)BTA film formed in Region I. Such an adsorption may be attributed to van der Waal's forces or pi stacking. Using the arguments presented above, the thickness of the film in Region III is 0.250, 0.575, and 1.24 μm in the presence of 5×10^{-4}, 5×10^{-3}, and 10^{-2} M BTAH, respectively.
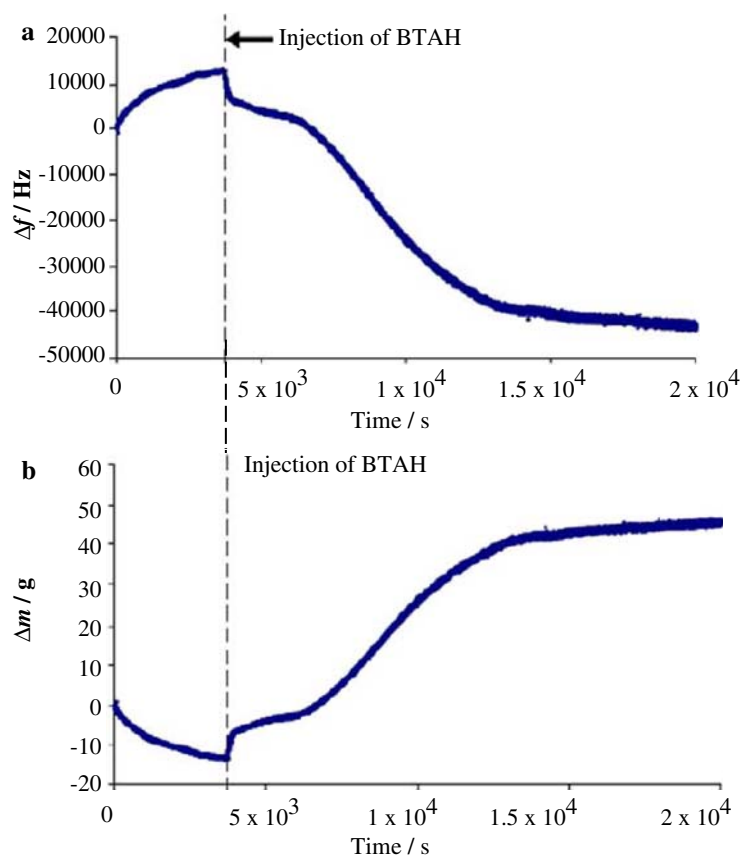
Fig. 2 Changes of resonant frequency (**a**) and mass of copper (**b**) in 3.5% NaCl before and after injection of BTAH into the electrolyte to establish a concentration of 5×10^{-3} M BTAH. The *vertical dashed line* marks the time of injection of BTAH

Fig. 3 Changes of resonant frequency (**a**) and mass of copper (**b**) in 3.5% NaCl before and after injection of BTAH into the electrolyte to establish a concentration of 1×10^{-2} M BTAH. The *vertical dashed line* marks the time of injection of BTAH
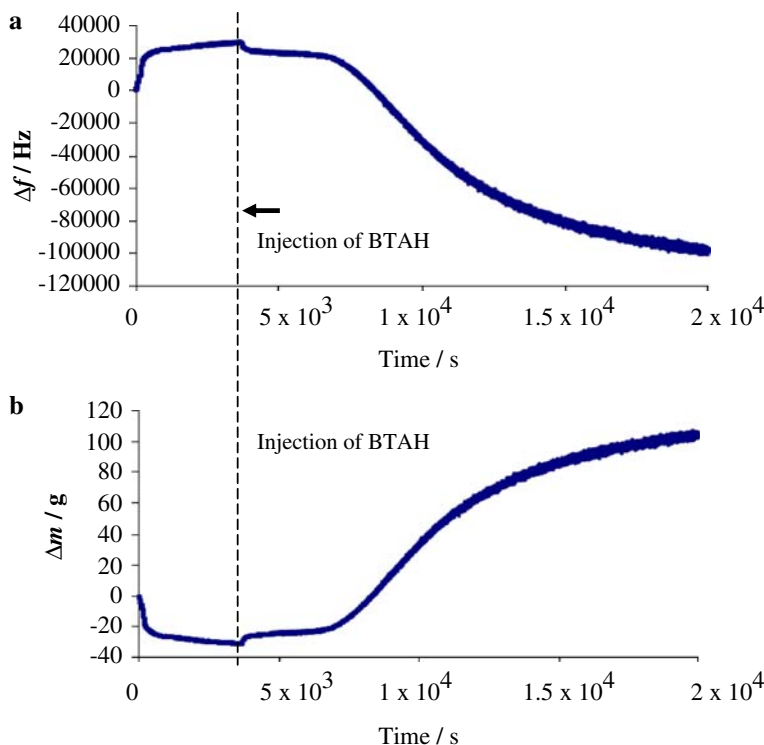
3.2 X-ray photoelectron spectroscopy

Figure 4 illustrates the N1s peak in the XPS spectra obtained from the copper surfaces after immersion in a solution containing 5×10^{-4} M BTAH for 10 min (curve a) and 3 h (curve b). The center of the peaks occurs at 399.5 eV which is characteristic of nitrogen (relative to a binding energy of 248.6 eV for C1s). The intensity of the peak at longer time is higher than that at short time, indicating a greater amount of BTAH on the surface as the immersion time increases.
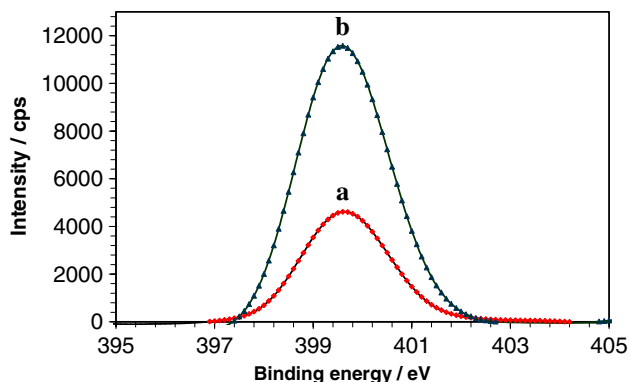
Upon sputtering the surface with an argon ion beam, the intensity of both peaks decrease with time as shown in Fig. 5. The rapid initial decrease in intensity with time is attributed to the facile removal of the physically adsorbed BTAH layer at the outer surface of the film. Subsequently, the intensity decreases with time at a much slower rate, which reflects a more stable film of Cu(I)BTA beneath the physically adsorbed layer of BTAH.
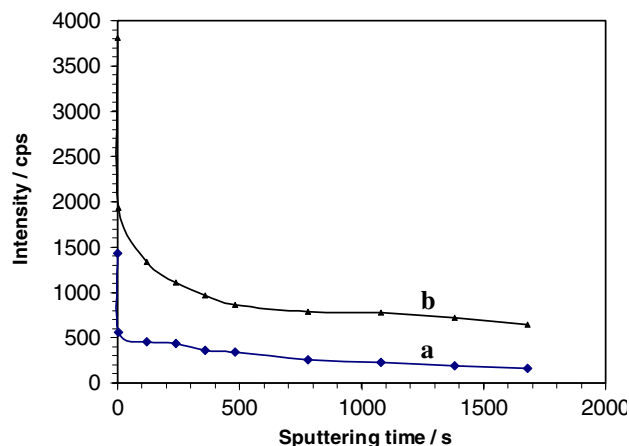

Fig. 4 The N1s peak in the XPS spectra of the copper surfaces after immersion in a medium containing 5×10^{-4} M BTAH for 10 min (**a**) and 3 h (**b**)

Fig. 5 Variation of the intensity of the N1s peak in the XPS spectra of the copper surface with the time of sputtering for the samples immersed for 10 min (**a**) and 3 h (**b**)

4 Conclusions

The mode of interaction of BTAH with the surface of corroding copper is described in terms of three regions. Region I shows rapid linear growth of the Cu(I)BTA complex with time. The thickness of the film that forms at the end of region I amounts to 540 Å, independent of the concentration of BTAH in the electrolyte. Region II shows further attachment of BTAH on the Cu(I)BTA film which forms on the surface, and hence gradual thickening of the film until a constant mass is reached (Region III), indicating the attainment of an equilibrium thickness of the film. The adsorption of BTAH during Region II on the Cu(I)BTA complex occurs at a slower rate. This is attributed to weak van der Waal forces and pi stacking between the pi electrons in the BTAH molecules. As the concentration of BTAH increases, the shape of Region II changes and the value of the plateau (Region III) increases, indicating a thicker film of BTAH under equilibrium condition.

The results offer an explanation for the much documented findings of simultaneous increase in polarization resistance and decrease in double layer capacity with time of immersion of copper in BTAH inhibited media [4, 16, 52]. They show clearly that these changes are directly related to the mass of BTAH attached to the copper surface.

References

1. Hashemi T, Hogarth CA (1988) Electrochim Acta 33(8):1123
2. Fox PG, Lewis G, Boden PJ (1979) Corros Sci 19(7):457
3. Cotton JB, Scholes IR (1967) Br Corros J London 2(1):1
4. Heakal FE, Haruyama S (1980) Corros Sci 20(7):887
5. Chan HYH, Weaver MJ (1998) Langmuir 15(9):3348
6. Polewska W, Vogt MR, Magnussen OM, Behm RJ (1999) J Phys Chem B 103(47):10440
7. Tromans D, Li G (2002) Electrochem Solid St Lett5(2):5
8. Schultz ZD, Biggin ME, White JO, Gewirth AA (2004) Anal Chem 76(3):604
9. Al-Hinai AT, Osseo-Asare K (2003) Electrochem Solid St 6(5):23
10. Hegde S, Babu SV (2003) Electrochem Solid St 6(10):G126
11. Tsai TH, Yen SC (2003) Appl Surf Sci 210(3, 4):190
12. Vogt BD, Lin EK, Wu WL, White CC (2004) J Phys Chem B 108(34):12685
13. Frignani A, Fonsati M, Monticelli C, Brunoro G (1999) Corros Sci 41(6):1217
14. Jin-Hua C, Zhi-Cheng L, Shu C, Li-Hua N, Shou-Zhuo Y (1997) Electrochim Acta 43(3, 4):265
15. Telegdi J, Shaban A, Kalman E (2000) Electrochim Acta 45(22):3639
16. Metikos-Hukovic M, Babic R, Marinovic A (1998) J Electrochem Soc 145(12):4045
17. Ravichandran R, Rajendran N (2005) Appl Surf Sci 239(2):182
18. Ravichandran R, Nanjundan S, Rajendran N (2004) J Appl Electrochem 34(11):1171
19. Papapanayiotou D, Deligianni H, Alkire RC (1998) J Electrochem Soc 145(9):3016
20. Tantavichet N, Pritzker M (2006) J Appl Electrochem 36(1):49
21. Scendo M, Malyszko J (2000) J Electrochem Soc 147(5):1758
22. Schmidt W, Alkire RC, Gewirth AA (1996) J Electrochem Soc 143(10):3122
23. Deshpande S, Kuiry SC, Klimov M, Obeng Y, Seal S (2004) J Electrochem Soc 151(11):G788; S. Deshpande, Kuiry SC, Klimov M, Seal S (2005) J Electrochem Solid St 8(4):G98
24. Li XJ, Guo DM, Ren RK, Jin ZJ (2006) In: Cai G, Xu X, Kang R (eds) Advances in grinding and abrasive technology XIII, key engineering materials, vol 304, 305. Trans Tech Publications, Switzerland, pp 350–354
25. Fang JY, Tsai MS, Dai BT, Wu SY, Feng MS (2005) Electrochem Solid St 8(5):G128
26. Babic-Samardzija K, Hackerman N (2005) J Solid St Electrochem 9(7):483
27. Sayed SY, El-Deab MS, El-Anadouli BE, Ateya BG (2003) J Phys Chem 107(23):5575
28. Cao PG, Yao JL, Zheng JW, Gu RA, Tian ZQ (2002) Langmuir 18(1):100
29. Brusic V, Frisch MA, Eldredge BN, Novak FP, Kanfman FB, Rush BM, Frankel GS (1991) J Electrochem Soc 138(8):2253
30. Fenelon AM, Breslin CB (2001) J Appl Electrochem 31(5):509
31. Walker R (1999) Br Corros J 34(4):304
32. Walsh JF, Dhariwal HS, Gutierrez-Sosa A, Finetti P, Muryn CA, Brookes NB, Oldman RJ, Thornton G (1998) Surf Sci 415(3):423
33. Jiang Y, Adams JB, Sun D (2004) J Phys Chem B 108(34):12851
34. Hegazy HS, Ashour EA, Ateya BG (2001) J Appl Electrochem 31(11):1261
35. Poling GW (1970) Corros Sci 10(5):359
36. Mansfield F, Smith T, Parry ET (1971) Corrosion 28(7):289
37. Clerc C, Alkire R (1991) J Electrochem Soc 138(1):25
38. Alkire R, Cangellari A (1989) J Electrochem Soc 136(4):913
39. Sauerbrey G (1959) Z Physik 155(206):206
40. Marx KA (2003) Biomacromolecules 4(5):1099
41. Zhou A, Xie B, Xie N (2000) Corros Sci 42(3):469
42. Mansikkamäki K, Ahonen P, Fabricius G, Murtomaki L, Kontturi K (2005) J Electrochem Soc 152(1):B12
43. Qafsaoui W, Blanc C, Pebere N, Takenouti H, Srhiri A, Mankowski G (2002) Electrochim Acta 47(27):4339
44. Hepel M, Cateforis E (2001) Electrochim Acta 46(24, 25):3801
45. Fonsati M, Zucchi F, Trabanelli G (1998) Electrochim Acta 44(2, 3):311
46. Kern P, Landolt D (2001) J Electrochem Soc 148(6):B228
47. Szocs E, Vastag Gy, Shaban A, Kalman E (2005) Corros Sci 47(4):893
48. Chmielova M, Seidlerova J, Weiss Z (2003) Corros Sci 45(5):883
49. Kear G, Barker BD, Walsh FC (2004) Corros Sci 46(1):109
50. Davies PR, Edwards D, Richards D (2004) Surf Sci 573(2):284
51. Warren MR, Madden JD (2006) Synthetic Met 156(9, 10):724
52. Al Kharafi FM, Ateya BG (2002) J Electrochem Soc 149(6):B206